Appl. Phys. B 79, 457–462 (2004)
DOI: 10.1007/s00340-004-1581-8

Applied Physics B
Lasers and Optics

K. FINSTERBUSCH✉
A. BAYER
H. ZACHARIAS

Tunable, narrow-band picosecond radiation in the mid-infrared by difference frequency mixing in GaSe and CdSe

Physikalisches Institut, Westfälische Wilhelms-Universität,
Wilhelm-Klemm-Str. 10, 48149 Münster, Germany

Received: 5 February 2004/Revised version: 14 May 2004
Published online: 20 July 2004 •

ABSTRACT We report on the generation of tunable, narrow-band picosecond laser pulses in the mid-IR at 1 kHz repetition rate. An optical parametric oscillator (OPO) seeded optical parametric amplifier (OPA) delivers signal and idler pulses with energies of several hundred microjoule tunable between 1.56 and 3.24 μm. Difference frequency mixing of the OPA signal and idler waves permits the generation of mid-IR radiation between 3 and 24 μm. The laser system therefore permits full coverage of the wavelength range between 1.6 and 24 μm. Conversion efficiencies greater than 50% and pulse energies up to 40 μJ are obtained with GaSe.

PACS 42.65.Re; 42.65.Yj; 42.72.Ai

1 Introduction

Sources of tunable high-quality, ultra-short laser pulses in the near- and mid-infrared spectral region are an important tool in various fields of optical spectroscopy. As far as comparatively compact sources are concerned the near and mid-IR (MIR) wavelength range up to 24 μm can be covered best by means of nonlinear frequency conversion. Extensive experimental studies have been carried out in this field of research in both the nanosecond and picosecond/femtosecond regime. For many experimental applications the picosecond time domain is optimal, because it offers a high spectral resolution while retaining a high conversion efficiency. Nonlinear materials like $AgGaSe_2$, GaSe and CdSe have been proven to be well suited in the considered wavelength range. Starting with intense but fixed-frequency radiation at 1 μm different conversion schemes depending on the pump system have been investigated. As GaSe allows for pumping at 1 μm efficient generation of MIR radiation is possible by parametric amplification of tunable near-IR (NIR) radiation delivered by dye lasers [1, 2] or parametric sources [3] with tuning ranges up to 20 μm. Recently Shi et al. [4] reported on phase-matched MIR generation in GaSe up to 28 μm by difference frequency mixing of a Nd:YAG laser (1.064 μm) and a tunable near NIR parametric source with ns pulse duration. A drawback of such a conversion scheme is the two-photon absorption (TPA) in GaSe still observable for high intensity radiation around 1 μm [5]. Therefore pumping at longer wavelengths seems to be a reasonable choice [6]. Unfortunately, there is a lack of commercially available high-power picosecond pump sources in the wavelength range above 1 μm working at repetition rates around 1 kHz, as it is advantageous for most experimental applications. To avoid problems with TPA in GaSe radiation in the mid-IR spectral region can be generated by difference frequency mixing (DFM) between the signal and idler waves of a parametric near-IR source. This scheme is then also applicable to CdSe which is not well suited for pumping at wavelengths shorter than ≈ 1.5 μm because of significant TPA. Despite this Shi et al. [7] applied the same scheme as mentioned above to CdSe and achieved phase-matched DFM in the range from 23 to 28 μm. The generation in the absorptive region limits, however, the conversion efficiency in both cases.

A compact OPO/DFM conversion chain was demonstrated first with nanosecond pulses by Bhar et al. [8] and adopted later for CdSe [9] and GaSe [10]. In the picosecond time domain efficient generation of high peak-power mid-IR pulses can be achieved by use of a seeded optical parametric amplifier (OPA) instead of an optical parametric oscillator (OPO). So far this was only demonstrated for CdSe [11, 12].

In this paper we report on the performance of a tunable source of picosecond laser pulses which completely covers the wavelength range between 1.56 and 24 μm via nonlinear IR generation in a 1 μm pumped OPO/OPA/DFM conversion chain operating at a repetition rate of 1 kHz. High photon conversion efficiencies of more than 50% are obtained with GaSe.

2 Experimental

The three stage conversion scheme is schematically shown in Fig. 1. The first stage consists of a 1053 nm pumped optical parametric oscillator (OPO) based on periodically poled lithium niobate (PPLN) [13]. The signal wave serves as narrow-band seed radiation for the following optical parametric amplifier (OPA) based on $KTiOPO_4$ (KTP) [14]. Finally the signal and idler waves of the OPA are difference frequency mixed in GaSe and CdSe. Tuning the OPA signal and idler waves between 1.56 and 3.24 μm permits mid-IR generation in the 3–24 μm range.

✉ Fax: +49-251/83-33604, E-mail: finster@uni-muenster.de

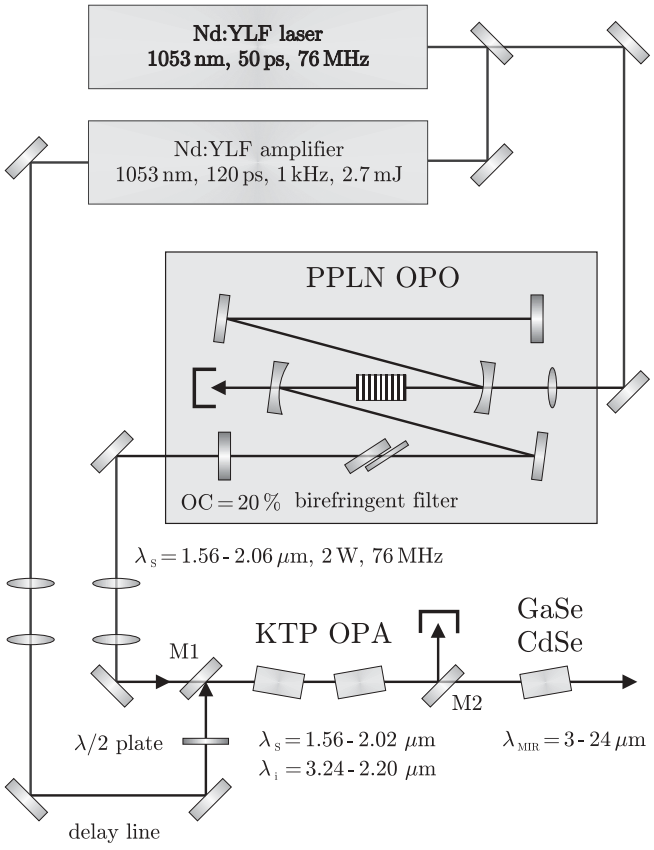

FIGURE 1 Schematic diagram of the experimental setup

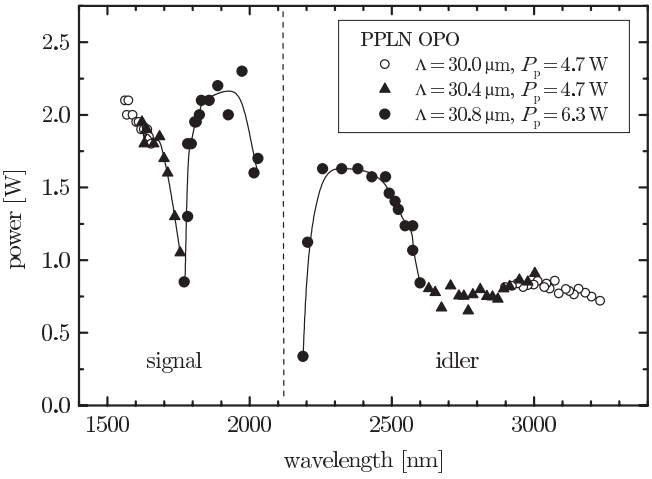

FIGURE 2 Typical signal and idler output power of the PPLN OPO using a 20% output coupler. The tuning range shown is covered by two sets of mirrors. The *solid line* is a guide to the eye

2.1 *The OPO stage*

The optical parametric oscillator (OPO) is pumped by a cw mode-locked Nd:YLF laser (Quantronix 4216 DL) which generates pulses at a wavelength of 1053 nm with a duration of 50 ps and a repetition rate of 75.7 MHz. Differing from an earlier report [13] the z-cavity of the OPO is arranged asymmetrically and contents a two-plate birefringent filter ensuring a long-term spectral stability of the emission [15]. Two different sets of mirrors are used. Mirror set I is highly reflective ($T < 0.5\%$) for the signal radiation in the wavelength range of 1.8–2.05 μm, and mirror set II covers a wavelength range of 1.5–1.75 μm. The 19 mm long multi-grating PPLN chip (Crystal Technology) has an aperture of $0.5 \times 11\,\mathrm{mm}^2$ and eight different poling periods between 30.0 and 31.2 μm. By changing the crystal temperature and using different poling periods the signal wave can be tuned from 1.56 to 2.06 μm corresponding to an idler tuning range of 2.15 to 3.24 μm. The tuning range is limited by the shortest available poling period on the chip and the restriction to crystal temperatures above 80 °C to avoid photorefractive damage of the crystal.

Figure 2 illustrates the tuning characteristic of the OPO. For mirror set I and a pump power of 6.3 W inside the crystal the average signal and idler output power is about 2.0 and 1.5 W, respectively, except at the limits of the reflectivity range. For mirror set II and a pump power of 4.7 W inside the crystal the average output power is about 1.8 W for the signal and 0.8 W for the idler wave. As the OPO operates at a repetition rate of 76 MHz the seed pulse energy is of the order of several nJ over the whole tuning range.

The nearly Fourier transform limited signal pulses have a duration of 45 ps and a spectral width of 11 GHz ($0.37\,\mathrm{cm}^{-1}$), resulting in a time-bandwidth product of $\Delta\tau \times \Delta\nu = 0.50$, which does not change significantly over the tuning range. After the seed beam is telescoped down to a beam radius of 0.7 mm it is overlapped with the pump beam of the OPA by dichroic mirror M1 (Fig. 1).

2.2 *The OPA stage*

The OPO seeded KTP OPA is pumped by a regenerative Nd:YLF amplifier generating Gaussian pulses at 1053 nm with an energy of about 2.7 mJ and a duration of 120 ps. The system operates at a repetition rate of 1 kHz. A 2:1 telescope provides a beam waist with a radius of 0.5 mm ($\mathrm{HW1/e}^2 M$) at the crystal positions, which leads to pump intensities of several $\mathrm{GW/cm}^2$.

Employing a 1053 nm pump the envisaged signal and idler tuning range of about 1.6–3.1 μm can completely be covered by both type IIa ($\mathrm{o} \rightarrow \mathrm{e} + \mathrm{o}$) and type IIb ($\mathrm{o} \rightarrow \mathrm{o} + \mathrm{e}$) phase matching in the xz-plane of KTP with phase matching angles of 45–51° and 51–75°, respectively. As the effective nonlinear coefficient for type II interaction is given by $d_{\mathrm{eff}} = d_{24} \sin\theta$, the nonlinear figure-of-merit (FOM), defined as $\mathrm{FOM} = d_{\mathrm{eff}}^2/n_p n_s n_i$, takes values between 0.65 and $1.22\,\mathrm{pm}^2/\mathrm{V}^2$ for phase matching angels between 45 and 75°, respectively, using a nonlinear coefficient of $d_{24} = 2.65\,\mathrm{pm/V}$ [16] and dispersion relations from [17]. In the same range of phase matching angels the birefringent walk-off decreases from 2.8 to 1.4°.

The KTP OPA reported in [14] is based on two uncoated 15 mm long KTP crystals with an aperture of $5 \times 5\,\mathrm{mm}^2$ cut at $\theta = 54°$ and $\varphi = 0°$ for type IIb phase matching in the xz plane. It is used in combination with mirror set I of the PPLN OPO for mid-IR generation in the 6–24 μm range. For shorter mid-IR wavelengths a type IIa KTP OPA is employed because of the much wider tunability compared to type IIb phase matching. However, the somewhat smaller FOM com-

bined with slightly greater walk-off may result in less efficient amplification. The type IIa OPA is used in combination with OPO mirror set II. The two uncoated KTP crystals are both 20 mm long with an aperture of $5 \times 6\,\text{mm}^2$ and cut at $\theta = 47°$.

The pump is separated from the OPA output beams by mirror M2 (Fig. 1), which shows a transmission between 75 and 98% depending on wavelength and polarization. Thus the wavelength dependence of the output pulse energies is affected by mirror M2. Figure 3 shows the usable signal and idler pulse energies for a pump energy of 2.7 mJ after separating-off the pump. The OPA signal and idler tuning ranges are similar to those of the PPLN OPO. Except at the limits of the tuning range of the seed radiation the signal and idler pulse energies range between 350 and 500 μJ and 200 and 400 μJ, respectively. The efficiency of the type IIb OPA is about 45% over a wide tuning range, whereas that of the type IIa OPA is about 30%. These values are derived from the input pump energy and the total OPA output energy taking only reflection losses at the front surface of the first crystal and rear surface of the second crystal into account. Thus the real quantum efficiency is even higher. The divergence of the OPA radiation has been measured for the idler wave to be about 4 mrad. The OPA signal pulses are three times the Fourier limit with an increased pulse duration of about 100 ps due to saturation and a spectral width of about 13 GHz ($0.43\,\text{cm}^{-1}$). Thus the signal bandwidth is similar to that of the seed pulses.

2.3 *The DFM stage*

After separating off the pump beam by dichroic mirror M2 (Fig. 1) the signal and idler beam of the OPA are difference frequency mixed in GaSe and CdSe. The crystals are placed 19 cm behind the OPA where the beam radii (HW1/e^2M) of the signal and idler waves are (0.8 ± 0.1 mm) and (1.29 ± 0.13 mm), respectively. No focusing optics are employed. The peak intensities of the signal and idler pulses then range between 330 and $470\,\text{MW/cm}^2$ and 70 and $140\,\text{MW/cm}^2$, respectively. Under these circumstances no crystal damage was observed for neither the GaSe nor the CdSe crystal during several months of operation.

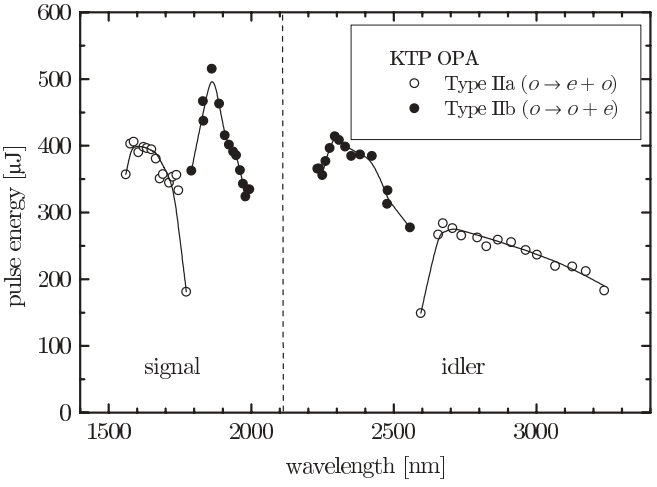

FIGURE 3 Signal and idler pulse energies of the 1053 nm pumped KTP OPA usable for DFM at a pump energy of 2.7 mJ. The *solid line* is a guide to the eye

Two z-cut GaSe crystals (Research Technology Instruments GmbH, Germany) with a length of 3.5 and 10 mm and a diameter of 10 mm are employed. The crystals are cleaved resulting in an optical surface quality that is not optimal but slightly bumpy. The transparency of the crystals is lowered by air gaps running from the rim to several millimeters inside the crystal. Thus one has to find a region of the crystal with high transparency and no distortion of the beam profile by surface bumpiness. As the effective nonlinear coefficients for type I and type II phase matching are given by [18]

$$d_{\text{eff}} = -d_{22} \cos\theta \sin 3\varphi \qquad \text{(type I)}, \tag{1}$$

$$d_{\text{eff}} = -d_{22} \cos^2\theta \cos 3\varphi \qquad \text{(type II)}, \tag{2}$$

the azimuthal angle φ has to be adjusted properly. Here φ was adjusted for optimal type I phase matching, which exhibits smaller phase matching angles and walk-off and slightly higher efficiency than type II. A nonlinear coefficient of $d_{22} = 54\,\text{pm/V}$ and dispersion relations given in [20] result in a FOM of about $120\,\text{pm}^2/\text{V}^2$ for type I interaction. For the considered mixing process the spectral acceptance is much larger than the bandwidth of the input pulses. But while the angle acceptance for the 3.5 mm long crystal of about 3 mrad is sufficiently large, an angle acceptance of only 1 mrad for the 10 mm crystal may affect the output energy.

Compared to GaSe the optical quality of the CdSe crystal (Cleveland Crystals) is excellent. The uncoated crystal is 12 mm long with an aperture of $5 \times 6\,\text{mm}^2$ cut at $\theta = 67°$ for type II phase matching. The effective nonlinearity is given by $d_{\text{eff}} = d_{31} \sin\theta$. A nonlinear coefficient of $d_{31} = -18\,\text{pm/V}$ and dispersion relations given in [20] result in a FOM of about $19\,\text{pm}^2/\text{V}^2$, which is about six times smaller compared to GaSe. For the considered mixing process both spectral and angle acceptance are sufficiently large.

The generated MIR pulses are characterized after separating off the signal and idler beam by a Ge filter with a 5% cut-on wavelength of 3.6 μm. The filter transmission is between 90 and 17% for wavelengths between 4 and 24 μm. The pulse duration is measured by cross-correlation between the pump and the MIR pulses in a GaSe crystal of 2 mm length. The spectral width is measured by a scanning Fabry–Pérot interferometer (FPI) with a variable mirror distance [19].

3 Results and discussion

3.1 *Difference frequency mixing in* GaSe

Figure 4 shows the transmission of the GaSe crystals in the discussed wavelength range measured with a Fourier transform spectrometer. The measurements have been carried out in air under atmospheric pressure in the case of the 3.5 mm long crystal and at a pressure of about 30 mbar in the case of the 10 mm long crystal. For wavelengths shorter than 8 μm the transmission of the 3.5 mm crystal is consistent with Fresnel losses at two surfaces showing that additional reflection losses caused by air gaps inside the crystals do not play a role. For longer wavelengths increasing crystal absorption lowers the transmission. The measured transmission at a wavelength of about 10 μm results in a linear absorption coefficient of about $0.14\,\text{cm}^{-1}$ compared to values of

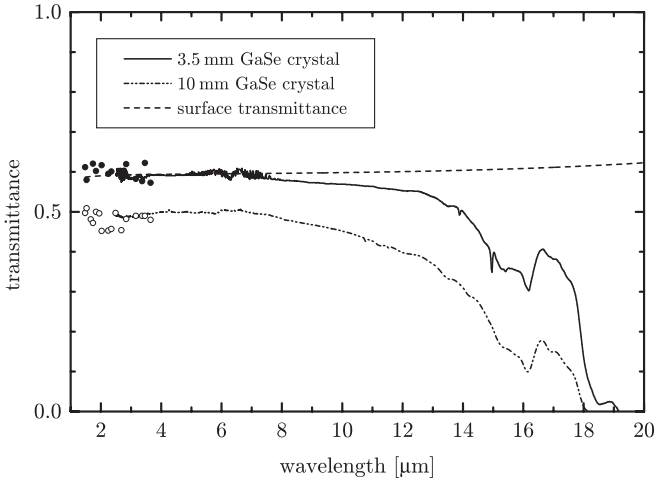

FIGURE 4 Measured transmittance for the 3.5 and 10 mm long GaSe crystals. The symbols indicate measurements carried out with the signal and idler beams of the PPLN OPO. *Solid dots*: 3.5 mm crystal, *open dots*: 10 mm crystal

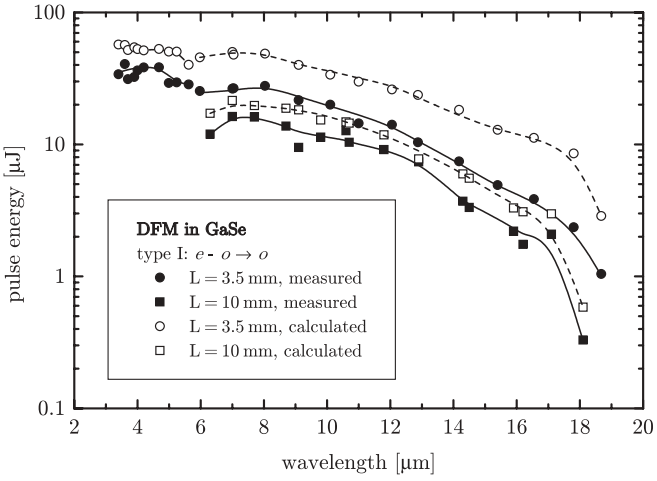

FIGURE 5 Output energy of the MIR pulses for DFM in GaSe (*solid symbols*). The *open symbols* correspond to theoretical values obtained by SNLO [22]. The *solid and dashed lines* are guides to the eye

0.05–0.081 cm^{-1} given in literature [20]. The spectral features between 4 and 8 μm are due to carbon dioxide and water absorption in air. The 10 mm crystal shows absorption over the whole wavelength range with increasing values for wavelengths above 8 μm. Additional to material absorption the transmission might be affected by the air gaps mentioned above. However, it can not be distinguished between material absorption and reflection losses caused by air gaps. The upper wavelength limits of the 3.5 and 10 mm long sample are 19 and 18 μm, respectively, somewhat shorter compared to known values from literature [18, 21]. Unfortunately there are no supplier specifications available. For wavelengths below 2.5 μm not accessible with the Fourier transform spectrometer the transmission of the GaSe crystals has been measured by use of the signal and idler radiation of the OPO down to 1.6 μm. The results are also shown in Fig. 4 as solid (open) dots for the 3.5 mm (10 mm) crystal. In the case of the 3.5 mm crystal the measured average transmission of 0.60 is consistent with Fresnel losses, whereas the 10 mm long crystal shows an average transmission of 0.48 in this wavelength range. The high-power transmittance has been measured at two different signal wavelengths of 1.92 and 1.95 μm and corresponding idler wavelengths of 2.33 and 2.29 μm, respectively, by use of the OPA radiation. No significant sign of two-photon absorption (TPA) has been detected at these wavelengths at peak intensities up to 300 MW/cm^2.

Figure 5 shows the output energy of the DFM stage. The values are corrected for the transmittance of the Ge filter. In the case of the 3.5 mm crystal the MIR radiation is tuned between 3.4 and 19 μm. The pulse energies range between a maximum of about 40 μJ at 4.0 μm and 1.0 μJ at 18.7 μm corresponding to 40 mW and 1 mW average power in the mid-IR, respectively. The quantum efficiency determined by depletion of the OPA signal wave is greater than 30% over the hole tuning range with maximum values over 50% around 4 μm. To our knowledge this is the highest efficiency reported for DFM in GaSe in the picosecond regime so far. Dahinten et al. [2] reported on 1053 nm pumped optical parametric amplification of NIR radiation in GaSe achieving maximum quantum efficiencies of about 2%. In a similar scheme Bayanov et al. [3] obtained a photon conversion efficiency of about 11% for both parametric amplification and difference frequency generation in GaSe pumped around 1 μm. For wavelength above 13 μm one finds an increasing discrepancy between the measured pulse energy and the energy expected from available signal pulse energy, wavelength and measured efficiency. This is due to the decreasing crystal transmission discussed above. The pulse energies obtained with the 10 mm crystal are somewhat lower and range between 16 μJ at 7 μm and 0.3 μJ at 18 μm. The 3–6 μm wavelength range was not measured for the 10 mm crystal. As in the case of the short sample the photon conversion efficiency is derived from depletion of the signal beam. In spite of the fact that the energies obtained with the long crystal are less than those obtained with the short one, the efficiency is similar to that measured for the 3.5 mm long sample with values ranging between 50 and 30% at 7 and 18 μm, respectively. There are two possible explanations for this fact. On the one hand the influence of crystal absorption at the signal wavelength of about 0.2 cm^{-1} leads to incorrect high values for depletion. On the other hand the MIR beam could be attenuated by crystal absorption.

Calculated values for the mid-IR pulse energies are also plotted in Fig. 5. The calculation was performed with the "2D-Mix-LP" tool of the SNLO software package [22] which accounts for spatial effects and linear absorption, but assumes the waves to be monochromatic and the pulses to be long enough that group velocity effects are unimportant. The two latter aspects are sufficiently well fulfilled in the present experiment. The largest difference between the group velocities of the signal, idler and MIR waves in the tuning range under consideration appears between the signal or idler and MIR pulse at a signal wavelength of 1990 nm corresponding to a MIR wavelength of 18 μm and amounts to about 0.5 ps/mm. Thus group velocity mismatch (GVM) does not play a role for 100 ps pulses. For each data point the individual input energies are used. In the calculations the signal and idler beam radii of (0.8 ± 0.1 mm) and (1.29 ± 0.13 mm), respectively, are kept constant over the whole wavelength

range. A nonlinear coefficient of $d_{22} = (54 \pm 11)$ pm/V is used and the spatial beam profile is assumed to be Gaussian. The values for linear losses in the crystals are deduced from the measured transmittance. As it can be seen from Fig. 5 the qualitative behaviour is reproduced. But the calculated values are too large by a factor of 2–3 for the 3.5 mm crystal and a factor of less than 2 for the 10 mm sample. However, as mentioned above the beam diameters and nonlinear coefficient are known within certain errors and the input energies are also measured with an uncertainty of about $\pm 50\,\mu$J. The uncertainty of the calculated output energies can roughly be estimated to $\pm 30\%$ by varying the input parameters within these limits. Additionally the quality of the input beam profiles is not well known. Nevertheless the calculation gives a possible explanation for the smaller output energies measured with the 10 mm crystal. With the given configuration a crystal length of 3–4 mm turned out to be optimal in the calculation, whereas the output energy is attenuated by back conversion when the crystal length is increased. Crystal absorption and angle acceptance seem to be less important.

At a wavelength of 11 μm the DFM pulses generated in the 3.5 mm long crystal have a duration of about $\Delta\tau = 90$ ps (FWHM). The bandwidth has been measured to $\Delta\nu = 14$ GHz ($0.47\,\mathrm{cm}^{-1}$). Again, the spectral width is not increased significantly, neither by parametric amplification nor by difference frequency mixing. Thus the time-bandwidth product is $\Delta\tau \cdot \Delta\nu = 1.2$, which is about three times the Fourier-transform limit and comparable to that of OPA signal and idler pulses.

The beam profile has been analyzed at a wavelength of 6.33 μm with a high-speed IR converter [23]. Figure 6 shows the intensity distribution in the focal plain of a 200 mm CaF_2 lens. The flat-top characteristic of the beam is clearly visible. The M^2 parameter [24] derived from such measurements yields $M_x^2 = 4.7$ in the x-direction (horizontal) and $M_y^2 = 3.4$ in the y-direction (vertical).

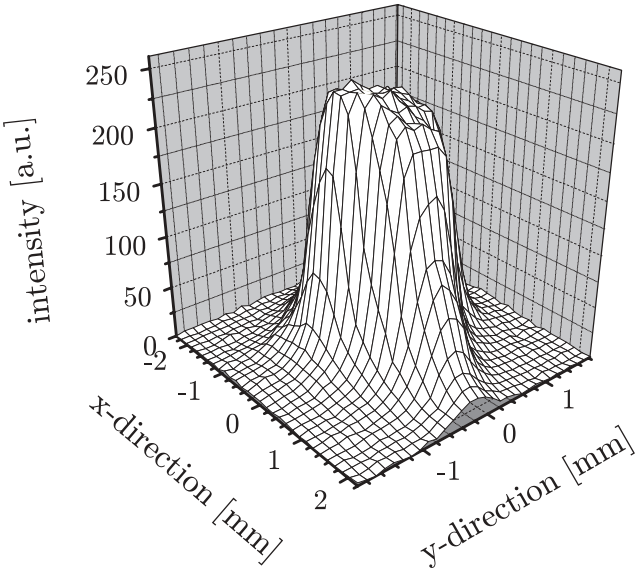

FIGURE 6 Spatial beam profile of the MIR radiation at a wavelength of 6.33 μm measured in the focal plane of a 200 mm CaF_2 lens

3.2 *Difference frequency mixing in* CdSe

Figure 7 depicts the transmission of the CdSe crystal which agrees well with Fresnel losses for wavelengths up to 16 μm. For longer wavelengths strong crystal absorption appears. In the signal and idler wavelength range under consideration, i.e. 1.90–2.37 μm, the low- and high-power transmittance has been measured as described above for GaSe and is consistent with Fresnel losses. As for GaSe no TPA is detected in CdSe.

Figure 8 shows the measured output energy of the DFM stage. Again the values shown are corrected for the transmission of the Ge filter. The MIR radiation can be tuned between 9 and 24.1 μm. The pulse energies range between a maximum of about 21 μJ at around 11 μm and 0.3 μJ at 24.1 μm corresponding to average powers of 21 mW and 0.3 mW, respectively. At a wavelength of 12 μm the pulse energy shows a significant drop for longer wavelengths. This fact can not be explained by absorption in the corresponding signal and idler wavelength range between 1.94 and 2.30 μm or attributed to

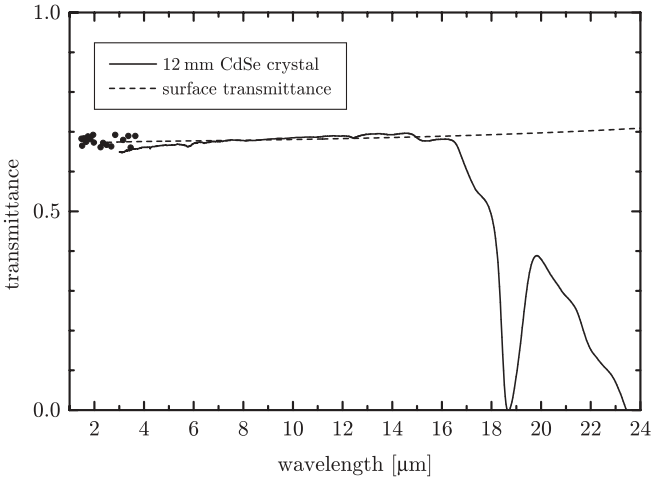

FIGURE 7 Measured transmittance for the 12 mm long CdSe crystal. The symbols indicate measurements carried out with the signal and idler beams of the PPLN OPO

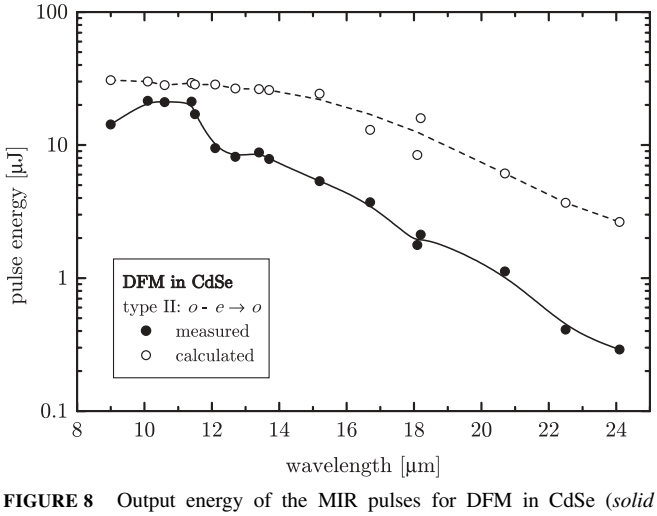

FIGURE 8 Output energy of the MIR pulses for DFM in CdSe (*solid symbols*). The *open symbols* correspond to theoretical values obtained by SNLO [22]. The *solid and dashed lines* are guides to the eye

any other crystal property. At present the reason for this behaviour is not known. The slightly steeper decrease of pulse energies for wavelength above 16 μm is due to increasing crystal absorption in this wavelength range. The photon conversion efficiency derived from the pulse energy of the OPA signal wave and the DFM wave inside the crystal is greater than 10% for wavelengths between 9 and 18 μm with maximum values of about 40% for wavelengths around 11 μm. In [12], Dhirani and Guyot-Sionnest reported on a similar scheme for the generation of picosecond pulses tunable in the 10 to 20 μm range with quantum efficiencies being higher than 50% from 10 to 18 μm. This might be due to higher input pulse energies and shorter pulse durations.

The calculated values for the MIR output energies also plotted in Fig. 8 are based on the same conditions as discussed above for GaSe. Again for wavelength between 10 and 12 μm the calculated output energies differ from the measured ones by a factor of two. With the exception of the drop in the measured pulse energy at 12 μm the qualitative behaviour is reproduced.

The generated DFM pulses are spectrally and temporally characterized at a wavelength of 11 μm. The pulse duration and bandwidth is about $\Delta\tau = 100\,\mathrm{ps}$ (FWHM) and $\Delta\nu = 15\,\mathrm{GHz}$ ($0.50\,\mathrm{cm}^{-1}$), respectively, giving a time-bandwidth product of $\Delta\tau \cdot \Delta\nu = 1.5$, which is about 3.4 times the Fourier-transform limit. The spectral width is only slightly broadened by a factor of 1.35 compared to the signal pulses of the PPLN OPO.

4 Summary

We reported on the generation of tunable, narrow bandwidth picosecond laser pulses in the mid-IR. A compact three stage conversion scheme is employed consisting of a 1053 nm pumped OPO/OPA system and a difference frequency mixing stage. The OPO seeded KTP OPA provides signal and idler pulses tunable between 1.56 and 3.24 μm with a small gap around degeneracy. The pulse energies amount to several hundreds of microjoules at 1 kHz repetition rate. Difference frequency mixing these pulses in GaSe and CdSe results in MIR pulses in the 3–24 μm wavelength range, so that most of the tuning range between 1.56 and 24 μm can be covered. Efficiencies greater than 50% are obtained with a 3.5 mm long GaSe crystal, which to our knowledge is the highest efficiency reported for DFM in GaSe in the picosecond regime so far. The pulse energies range between a maximum of 40 μJ at 4.0 μm and 1.0 μJ at 18.7 μm at 1 kHz. In the case of CdSe the MIR pulses can be tuned between 9 and 24.1 μm with pulse energies range between a maximum of 21 μJ at 11 μm and 0.3 μJ at 24.1 μm.

ACKNOWLEDGEMENTS This research was supported by the German Bundesministerium für Bildung, Wissenschaft, Forschung und Technologie under contract 13 N 7068.

The authors wish to thank S. Matern and V.M. Marchenko for providing the high-speed IR converter.

REFERENCES

1 J.L. Oudar, P.J. Kupecek, D.S. Chemla: Opt. Commun. **29**, 119 (1979)
2 T. Dahinten, U. Plödereder, A. Seilmeier, K.L. Vodopyanov, K.R. Allakhverdiev, Z.A. Ibragimov: IEEE J. Quantum Electron. **QE-29**, 2245 (1993)
3 I.M. Bayanov, R. Danielius, P. Heinz, A. Seilmeier: Opt. Commun. **113**, 99 (1994)
4 W. Shi, Y.J. Ding, X. Mu, N. Fernelius: Appl. Phys. Lett. **80**, 3889 (2002)
5 K.L. Vodopyanov, S.B. Mirov, V.G. Voedin, P.G. Schunemann: Opt. Commun. **155**, 47 (1998)
6 K.L. Vodopyanov: J. Opt. Soc. Am. B **16**, 1579 (1999)
7 W. Shi, Y.J. Ding: Opt. Commun. **207**, 273 (2002)
8 G.C. Bhar, D.C. Hanna, B. Luther-Davies, R.C. Smith: Opt. Commun. **6**, 323 (1972)
9 D.C. Hanna, B. Luther-Davies, R.C. Smith, R. Wyatt: Appl. Phys. Lett. **25**, 142 (1974)
10 A. Bianchi, A. Ferrario, M. Musci: Opt. Commun. **25**, 256 (1978)
11 A.J. Campillo, R.C. Hyer, S.L. Shapiro: Opt. Lett. **4**, 325 (1979)
12 A. Dhirani, P. Guyot-Sionnest: Opt. Lett. **20**, 1104 (1995)
13 K. Finsterbusch, R. Urschel, H. Zacharias: Appl. Phys. B **70**, 741 (2000)
14 K. Finsterbusch, R. Urschel, H. Zacharias: Appl. Phys. B **74**, 319 (2002)
15 D.R. Preuss, J.L. Gole: Appl. Opt. **19**, 702 (1980)
16 B. Boulonger, J.P. Feve, G. Marnier, B. Menaert, X. Cabirol, P. Villeval, C. Bonnin: J. Opt. Soc. Am. B **11**, 750 (1994)
17 H. Vanherzeele, J.D. Bierlein, F.C. Zumsteg: Appl. Opt. **27**, 3314 (1988)
18 G.B. Abdullaev, L.A. Kulevskii, A.M. Prokhorov, A.D. Savel'ev,break E.Y. Salaev, V.V. Smirnov: JETP Lett. **16**, 90 (1972)
19 S. Marzenell, R. Beigang, R. Wallenstein: Appl. Phys. B **71**, 185 (2000)
20 V.G. Dmitriev, G.G. Gurzadyan, D.N. Nikogosyan: *Handbook of Nonlinear Optical Crystals* (Springer-Verlag Berlin Heidelberg 1997), p. 166
21 K.L. Vodopyanov, L.A. Kulevskii, V.G. Voevodin, A.I. Gribenyukov, K.R. Allakhverdiev, T.A. Kerimov: Opt. Commun. **83**, 322 (1991).
22 SNLO nonlinear optics code available from A.V. Smith, Sandia National Laboratories, Albuquerque, NM 87185-1423.
23 S. Matern, V.M. Marchenko, H.-G. Purwins: Photonik **3**, 84 (2002)
24 O. Svelto: *Principles of Lasers* (Plenum Press, New York and London, 1998), p. 480